Biomaterials 258 (2020) 120285

Contents lists available at ScienceDirect

Biomaterials

journal homepage: www.elsevier.com/locate/biomaterials

The conductive function of biopolymer corrects myocardial scar conduction blockage and resynchronizes contraction to prevent heart failure

Sheng He [a,b], Jun Wu [a], Shu-Hong Li [a], Li Wang [c], Yu Sun [c], Jun Xie [b], Daniel Ramnath [a], Richard D. Weisel [a,e], Terrence M. Yau [e], Hsing-Wen Sung [d], Ren-Ke Li [a,e,*]

[a] Toronto General Hospital Research Institute, University Health Network, Toronto, Ontario, Canada
[b] Department of Biochemistry and Molecular Biology, Shanxi Key Laboratory of Birth Defect and Cell Regeneration, Department of Radiology, the First Hospital of Shanxi Medical University, Taiyuan, China
[c] Department of Mechanical and Industrial Engineering, University of Toronto, Toronto, Ontario, Canada
[d] Department of Chemical Engineering and Frontier Research Center on Fundamental and Applied Sciences of Matters, National Tsing Hua University, Hsinchu, Taiwan, ROC
[e] Division of Cardiovascular Surgery, Department of Surgery, University Health Network and University of Toronto, Toronto, Canada

ARTICLE INFO

Keywords:
Conductive biomaterial
Resynchronization
Myocardial infarction
Heart failure

ABSTRACT

Myocardial fibrosis, resulting from ischemic injury, increases tissue resistivity in the infarct area, which impedes heart synchronous electrical propagation. The uneven conduction between myocardium and fibrotic tissue leads to dys-synchronous contraction, which progresses towards ventricular dysfunction. We synthesized a conductive poly-pyrrole-chitosan hydrogel (PPY–CHI), and investigated its capabilities in improving electrical propagation in fibrotic tissue, as well as resynchronizing cardiac contraction to preserve cardiac function. In an *in vitro* fibrotic scar model, conductivity increased in proportion to the amount of PPY-CHI hydrogel added. To elucidate the mechanism of interaction between myocardial ionic changes and electrical current, an equivalent circuit model was used, which showed that PPY-CHI resistance was 10 times lower, and latency time 5 times shorter, compared to controls. Using a rat myocardial infarction (MI) model, PPY-CHI was injected into fibrotic tissue 7 days post MI. There, PPY-CHI reduced tissue resistance by 30%, improved electrical conduction across the fibrotic scar by 33%, enhanced field potential amplitudes by 2 times, and resynchronized cardiac contraction. PPY-CHI hydrogel also preserved cardiac function at 3 months, and reduced susceptibility to arrhythmia by 30% post-MI. These data demonstrated that the conductive PPY-CHI hydrogel reduced fibrotic scar resistivity, and enhanced electrical conduction, to synchronize cardiac contraction.

1. Introduction

Myocardial infarction (MI) is a major clinical problem worldwide, which can lead to progressive cardiac dysfunction and heart failure. Using current therapies, more than 80% of patients survive acute MI. However, the infarct results in cardiomyocyte (CM) necrosis, which is replaced by a fibrotic scar [1–3]. The fibrous tissue in the myocardium increases electrical resistance, which can result in delayed electrical propagation, leading to some regions of the heart being unable to contribute to blood propulsion from that organ. Cardiac resynchronization therapy has been shown to reduce mortality in heart failure patients, as well as those with low left ventricular ejection fractions and prolonged QRS intervals [4–6]. However, limitations of this technology have been identified, such as some patients requiring resynchronization being unable to achieve it [7]. Therefore, novel approaches are required to achieve synchronous contraction in these patients.

Conductive materials are polymers characterized by their ability to facilitate electric conductivity [8]. These materials contain a unique single- and double-bond structure, allowing inter-chain hopping of electrons. Although the conductive function of these polymers had been identified 2 decades ago, they have not been used in biological tissue repair, owing to their mechanical rigidity and non-biocompatibility [9]. To improve the biocompatibility of the polymers, we recently conjugated pyrrole onto a biological molecule, chitosan (CHI), and elongated

* Corresponding author. Division of Cardiovascular Surgery, Toronto General Hospital Research Institute, University Health Network, 101 College Street, Toronto, Ontario, M5G 1L7, Canada.
E-mail address: renkeli@uhnresearch.ca (R.-K. Li).

https://doi.org/10.1016/j.biomaterials.2020.120285
Received 4 February 2020; Received in revised form 24 June 2020; Accepted 1 August 2020
Available online 3 August 2020
0142-9612/© 2020 Elsevier Ltd. All rights reserved.

the pyrrole chain to synthesize a poly-pyrrole-chitosan (PPY–CHI) hydrogel, which is non-toxic, biocompatible and conductive [10,11].

Since the reason for cardiac dys-synchronous contraction is due to the delayed conduction velocity within myocardial fibrotic tissue, we investigated the feasibility of the PPY-CHI conductive polymer to re-circuit myocardial conduction and synchronize cardiomyocyte electrical activation. In our *in vitro* model, we found that PPY-CHI was able to bridge isolated cardiomyocytes to induce synchronous contractions. To elucidate the mechanism through which PPY-CHI facilitates the conversion from myocardial ionic changes to electrical current, thereby allowing the propagation of electrical signals across the non-conductive fibrotic scar, we established an equivalent circuit model and carried out impedance measurements. We found that PPY-CHI interface was easier to polarize, allowing for more effective conduction of the electrical signals generated by the myocardial tissue. Our *in vivo* studies showed that the biomaterial decreased fibrotic tissue resistivity, and enhanced the conductive velocity, of the injured myocardial tissue. Functional analysis showed that animals treated with PPY-CHI displayed improved cardiac function, and fewer cardiac arrhythmias, following restoration of tissue conduction.

2. Materials and methods

2.1. Biomaterial synthesis

A chemical oxidative polymerization method was used for PPY-CHI (3:10 ratio) hydrogel synthesis. Sixty μl of 98% pyrrole (Cat#: 131709, Sigma) was added to 10 ml of 2% CHI (Cat#: 448869, Sigma) acid solution, which was mixed by gentle swirling. $FeCl_3{\cdot}6H_2O$ (0.18 g, Cat#: 236489, Sigma) was then added to the solution, and mixed for 48 h for oxidative polymerization. A dialysis membrane (Cat#: 132700, Fisher Scientific) was used to remove un-polymerized pyrrole and free Fe. CHI (2%) was used as a control. Glycerol phosphate disodium (Cat#: G9422, Sigma) was used to adjust the pH of both PPY-CHI and CHI to 6.0. Glutaraldehyde (Cat#: G6257, Sigma) was used to form hydrogel.

2.2. Conductivity measurement

The conductivity of PPY-CHI and CHI hydrogels was evaluated using a 2-probe conductive analyzer (Hewlett-Packard Development Company, Palo Alto, CA). CHI and PPY-CHI hydrogels were both placed on a platform, and two probes at 7 mm distance from each other were used for conductivity measurements using a linear double-sweep model. The voltage was increased from −5 to +5 V in 100 mV increments (compliance 10 mA for 2 s, delay time 100 μsec). Conductivity was calculated according to the slopes.

Microelectrode array (MEA) was also used to evaluate biomaterial field potential amplitudes, at different distances from the voltage stimulation site. At the 0 cm mark, negative and positive prongs from a STG 4002 electric stimulator (Multi Channel Systems, Reutlingen, Germany) were placed on the biomaterial. MC stimulus II software (Multi Channel Systems, Reutlingen, Germany) was used to control the electrical stimulator voltage, in order to apply an electrical pulse of 400 mV every second. Cardio 2D + software (Multi Channel Systems, Reutlingen, Germany) was used to measure the electrical response detected by the MEA, for 10–15 s after the start of electrical stimulation. The recording prongs then were moved to distances of 1, 2, and 4 cm, where MEA recordings were taken at each distance under a constant stimulation voltage of 400 mV (1 pulse/sec). To measure fibrotic tissue model conduction *in vitro*, we used different gelatin concentrations (10–80% by volume) in the biomaterial, and used the MEA system to quantify bioconductivity. We measured any change in the electrical response magnitude, as the biomaterial composition was altered. MC stimulus II software was used to apply a 400 mV electrical pulse every second to the different biomaterial samples, each had an increasing biomaterial concentration and a decreasing gelatin concentration. Cardio 2D + software was used to analyze each recording.

2.3. Measurement of frequency response and establishment of equivalent circuit model

Impedance data includes a real and a simulated part (Equation (1) in supplementary material), which were used to decouple the values of biomaterials, MEA, biomaterial-MEA interface, and heart-biomaterial interface in the equivalent circuit model (Fig. 2a) of the heart-biomaterial-MEA composite.

Biomaterial impedance measurement: Gelatin or PPY-CHI hydrogel, with dimensions 14 mm × 14 mm × 5 mm, was used. Biomaterial impedance raw data was recorded by a resistivity apparatus (HF2IS, Zurich Instruments, Switzerland), and calculated by Equations (1) and (2) in supplementary material. When the frequency approaches infinity, the impedance magnitude is approximately the same as the resistance value (Equation (5) in supplementary material). Gelatin and PPY-CHI electrical resistivity was calculated by Equation (8) in supplementary material. In the two experimental groups (PPY–CHI and gelatin), the same thickness ($l = 5$ mm) and effective area ($A = 196$ mm^2) were used for both biomaterial types.

MEA impedance measurement: MEA impedance raw data was recorded by a resistivity apparatus, and plotted by Bode (Supplementary Fig. 1a) and Nyquist (Supplementary Fig. 1b). The plot shows that impedance magnitude remains largely constant throughout the frequency range, and the corresponding resistance plot shows points fluctuating around 195 kΩ. Thus, MEA was modeled as a resistor with the resistance value of 195 kΩ (RMEA in Fig. 2a).

Biomaterial-MEA interface impedance measurement: Gelatin or PPY-CHI hydrogel, with dimensions 14 mm × 14 mm × 5 mm, was placed on top of MEA, and the biomaterial-MEA interface impedance was recorded by a resistivity apparatus. The resulting data points were plotted by Nyquist. Biomaterial-MEA interface electrical resistivity was calculated by Equations (9)–(11), outlined in the supplementary material.

Heart-biomaterial interface impedance measurement: The heart was placed on biomaterials at dimensions 14 mm × 14 mm × 5 mm; the heart-biomaterial interface impedance was then recorded by a resistivity apparatus, and plotted by Nyquist. Heart-biomaterial interface electrical resistivity was calculated by Equations (9)–(11), as described in the supplementary material.

2.4. Acute MI model and biomaterial injection

Female Sprague Dawley (SD) rats (230–260 g) were purchased from Charles River Laboratories (Saint-Constant, QC, Canada). All animal protocols and procedures were approved by the Animal Care Committee of the University Health Network. Experimental procedures in the animal studies were performed in accordance to the Guide for the Care and Use of Laboratory Animals (NIH, 8th Edition, 2011). Rats were mechanically ventilated and anesthetized with 2% isoflurane. A left lateral thoracotomy was made to expose the heart, and the left anterior descending coronary artery was ligated to create a myocardial infarction (MI). The chest was then closed, and animals were given buprenorphine (0.05 mg/kg) for analgesia. All animals were randomized into saline, CHI or PPY-CHI injection groups. One week post-MI, a second thoracotomy was performed to access the heart, where the ventricular scar was visualized as a white-grey area on the anterior wall of the left ventricle. One hundred μL of saline, CHI, or PPY-CHI was injected into the middle layer of the myocardium at 3 sites (~33 μL/site), one in the center of the scar and two at the border regions on each side using a 28-gauge needle (BD Biosciences, Mississauga, ON). The chest was then closed and animals were given buprenorphine (0.05 mg/kg) for analgesia. All animals were sacrificed 12 weeks after biomaterial injection for optical mapping experiments.

2.5. Cardiac electrophysiology

We used four methods to evaluate cardiac electrophysiology. 1) Surface electrocardiograms [ECGs] (PowerLab 4/35, AD Instruments, Colorado Springs, Colorado) were recorded at baseline before infarction (−1 week), one week after infarction at the biomaterial injection time (week 0), as well as 2, 4, 6, 8, 10 and 12 weeks after injection (n = 8). We compared heart rate, QRS and QT intervals at each of the time points among the three groups. 2) Telemetric ECGs were performed at 12 weeks after injection (n = 4), and we counted the number of spontaneously-occurring arrhythmias each hour. 3) *In vivo* programmed electrical stimulation (PES) was used to evaluate induced arrhythmias upon the termination of the study. 4) We also used an eight-lead catheter ECG recording method and MEA to evaluate global and regional cardiac surface field potentials.

2.6. Cardiac tissue resistance measurement

We used a four-probe method to measure scar area resistance *ex vivo,* at the termination of the study. At the 12-week end point, animals were euthanized, and cardiac diastolic arrest was achieved by infusing a cardioplegic solution. Hearts were preserved in Krebs-Henseleit solution, and resistance was measured within 30 min. The four electrode probes, connecting to a resistivity apparatus, were inserted into the LV scar area at a depth of 1 mm. The distance between each electrode probe was 2.5 mm, and each probe was inserted into the scar area at the same depth. Probes 1 and 4 supplied a lower current that was not recorded, while recordings were taken for the voltage between probes 2 and 3. Resistance was calculated as the voltage between probes 2 and 3, divided by the current.

2.7. Cardiac left ventricular function

Cardiac function was evaluated using 2 techniques. 1) Echocardiography (Vivid7, General Electric Healthcare, Fairfield, Connecticut) before infarction (−1 week), at the time of biomaterial injection (week 0), as well as 2, 4, 6, 8, 10, and 12 weeks after injection. 2) Pressure–volume (P–V) analysis was conducted at the 12-week end point. The following parameters were calculated by echocardiography: left ventricular internal systolic dimension (LVIDs), left ventricular (LV) internal diastolic dimension (LVIDd), percentage of fractional shortening (LVFS) and percentage of ejection fraction (LVEF). P–V analysis was used to determine ejection fraction, dP/dt, tau, and LV volumes.

2.8. Optical mapping

At the 12-week end point, animals were euthanized, and heart contraction was stopped using a cardioplegic solution. Hearts were perfused using the Langendorff apparatus (120142, Radnoti, Monrovia, California) on ice, with cardioplegic solution and voltage-sensitive dye (di-4-ANEPPS, D1199, Life Technologies), for 10 min. Electrical conduction was measured using an electron-multiplied charge-coupled device camera system (Evolve 128, Photometrics, Tucson, Arizona), and isochronal maps were created. Videos were analyzed using Brainvision software (1312, Brainvision Inc. Tokyo, Japan).

2.9. Telemetric ECG

ECG recordings were acquired from conscious, freely mobile animals using a Millar telemetry system (Millar Inc., Houston, Texas). All recordings were obtained over a 24-h period from animals injected with PPY-CHI, CHI, or saline at 12 weeks post-injection. All ECG traces were evaluated by a blinded cardiologist using Histogram software (Millar Inc.), who determined the total number and frequency of arrhythmic events, including single and multiform premature ventricular contractions (PVCs), as well as non-sustained and sustained ventricular tachycardia (VT). In accordance with the Lambeth convention guidelines [12], VT was defined as a run of four or more PVCs, and sustained VT as a fast ventricular rhythm of >15 beats.

2.10. Programmed electrical stimulation

Programmed electrical stimulation (PES) studies were performed 12 weeks post-injection, using methods modified from Nguyen et al. [13]. In brief, each animal was mechanically ventilated and anesthetized with 2% isoflurane. Surface ECGs were recorded using a 27-gauge subcutaneous electrode, connected to a computer through an analog-digital converter, for monitoring and subsequent offline analysis (Lab Chart 6 Pro, AD Instruments, Colorado Springs, Colorado). A midline incision was made in the sternum, the chest was opened, and the heart epicardial surface exposed. Two epicardial stimulating electrode needles (Millar Inc.) were inserted into the surface of the right ventricular outflow tract, and recordings were made at the left ventricular apex. PES studies were then performed using an isolated stimulator-generator (STG-4002, Multichannel Systems, Germany). We employed standard clinical PES protocols, including burst (120 ms cycle length), single (70 ms cycle length), double (60 ms cycle length), and triple (50 ms cycle length) extra stimuli applied under spontaneous rhythms. The heart was challenged three times with the train of eight, or followed by the single extra-stimulus. If no arrhythmia was induced, this procedure was repeated to apply three challenges with double and, if necessary, triple extra stimuli. PES protocols were stopped if arrhythmia was induced, or until the protocol was exhausted. PVC or VT was induced in all infarcted animals with the application of a train of eight conditioning stimuli only, or up to a triple extra stimulus. Arrhythmia susceptibility was determined using an inducibility quotient as follows: Hearts with no PVCs or VT received a score of 0, non-sustained PVCs or VT (≤15 beats) induced with three extra stimuli were given a score of 1, sustained PVCs or VT (>15) induced with three extra stimuli were given a score of 2, non-sustained PVCs or VT induced with two extra stimuli were given a score of 3, sustained PVCs or VT induced with two extra stimuli were given a score of 4, non-sustained PVCs or VT induced with one extra stimulus were given a score of 5, sustained PVCs or VT induced with one extra stimulus were given a score of 6, sustained or non-sustained PVCs or VT induced after the train of eight were given a score of 7, and asystole after termination of pacing was given a score of 8. The higher the score, the greater the arrhythmia present.

2.11. Immunofluorescence staining

Formalin-fixed, paraffin-embedded rat heart slices were dewaxed and rehydrated. The slices were then permeabilized with 0.2% Triton X-100 in PBS and blocked for 1 h in PBS containing 10% bovine serum albumin. They were then incubated with primary antibody α-SMA (smooth muscle actin, Cat#: A2547, 1:800, Sigma) overnight at 4 °C. Incubation with Alexa546 donkey anti-mouse (Cat#: A10036, 1:400, Invitrogen) secondary antibody was carried out at room temperature for 1 h. The nuclei were identified with DAPI (Cat#: D9524, 1:2000, Sigma).

2.12. Statistical analysis

Data were expressed as mean ± standard deviation. Analyses were performed using GraphPad Prism software (v. 6.0), with the critical α-level set at $p < 0.05$. Student's *t*-tests were used for comparisons of means between two groups. Comparisons of means among three or more groups were performed using one-way analysis of variance (ANOVA). For ECG and echo analyses, which evaluated the same animals at different time points, repeated-measures ANOVA was employed. When the ANOVA F values were significant, differences between groups were determined using Tukey's *post-hoc* tests.

3. Results

3.1. Conductive biomaterial increased electrical conduction of fibrotic tissue in vitro

Using a two-probe measurement method, we demonstrated that PPY-CHI had significantly higher conductivity than CHI alone (Fig. 1a and b). The field potential of PPY-CHI was significantly greater than that of CHI, when measured by a MEA at 0.5, 1, and 1.5 cm from the electrodes (Fig. 1c). To assess the ability of PPY-CHI to reduce fibrotic tissue impedance, we generated a fibrotic tissue matrix *in vitro* using gelatin, and then introduced PPY-CHI to the fibrotic matrix (10–80% by volume). There, the fibrotic tissue (gelatin) matrix had the greatest resistance. PPY-CHI addition increased tissue conductivity, and this increase was found to be correlated with the PPY-CHI percentage (Fig. 1d). These data suggested that conductive PPY-CHI was able to reduce impedance and improve electrical conduction in a fibrotic tissue-like environment. Chitosan, as a widely used biomaterial for physiological applications, has some beneficial effects on conductivity and cardiac function. Chitosan has conductive characteristics ($\sim 2 \times 10^{-4}$ S/cm). However, its conductive property is lower than that of normal myocardium (6×10^{-4} S/cm) [14] The addition of conductive polymer PPY to CHI increased the conductivity by ~3 times, which is comparable to the conductivity of healthy myocardium. Therefore, PPY-CHI is an optimal biomaterial, being able to more effectively improve electrical propagation across the scar tissue. This improved conduction may ultimately result in the preservation of cardiac function.

In the myocardium, biological conduction is propagated by ionic (Na^+, K^+ and Ca^{2+}) currents. PPY-CHI acted as a "wire" to restore conductive propagation. It is important to elucidate the mechanism by which PPY-CHI is able to facilitate the conversion from myocardial ionic to electrical current, thus allowing the propagation of electrical signals across normally non-conductive fibrotic scar tissue. We performed *in vitro* studies to evaluate the interactions between PPY-CHI and cardiac cells/tissue, using the non-stimulated heart. We created a sealed system with a Langendorff-perfused beating heart on one side, and a MEA on the other side of a gelatin matrix cushion mimicking the fibrotic tissue (Fig. 1e). When the matrix cushion was purely gelatin and placed between a beating heart and the MEA, biological (electrical) conduction was barely detectable by MEA. As the percentage of PPY-CHI within the gelatin matrix cushion was increased, the field potential amplitude detected by MEA increased in a dose-dependent manner (Fig. 1f). PPY-CHI had a 10-fold higher field potential amplitude compared to CHI (Fig. 1g). This result suggested that an ionic current generated by a beating heart was able to stimulate an electrical current passing through the conductive polymer, which was detected by the MEA as voltage.

3.2. Quantification of the electrical parameters between the conductive and non-conductive biomaterials

To quantify the differences in electrical parameters between conductive (PPY–CHI) and non-conductive (gelatin) biomaterials, impedance measurements were carried out, and an equivalent circuit model was established (Fig. 2a). We investigated the energy decrease and latency time of an electrical current, when passing through each biomaterial in an equivalent circuit. Power spectrum analysis was performed to evaluate the energy distribution of signals at each frequency. As shown in Fig. 2b, the electrical current energy was largely distributed in the low-frequency range (<25 Hz). In addition, although decreases occurred in both PPY-CHI and gelatin, the energy that remained after passing through PPY-CHI at 1 Hz was 2.04 times greater than that passing through gelatin (Fig. 2b). The latency time was 1.83 ms for PPY-CHI and 9.87 ms for gelatin (Fig. 2c), indicating that the conduction velocity of an electrical current passing through PPY-CHI was significantly faster than that passing through the scar tissue-mimicking gelatin. These results suggested that energy loss in PPY-CHI was significantly lower compared to gelatin, implying that PPY-CHI helps to reduce the impact of fibrotic scarring by improving electrical current energy transfer.

The impedance and frequency response of biomaterials, MEA, MEA-biomaterial, and heart-biomaterial-MEA composite were separately measured, as shown in respective Bode and Nyquist plots (Fig. 2d and e). The frequency response of each biomaterial was measured from 100 Hz to 100 kHz with an applied voltage of 100 mV. Fig. 2d showed that the gelatin impedance magnitude was higher than that of PPY-CHI throughout the frequency range. For each frequency, the real and simulated components of the impedance response (Nyquist plot in Fig. 2e) were used to determine the electrical element values in the equivalent circuit model. Since PPY-CHI and gelatin frequency responses revealed linear profiles with different slopes, the equivalent circuit of both biomaterials can be represented as a resistor connected in series with a constant phase element [CPE] [15]. PPY-CHI fitted resistance was 344.50 Ω (R-square = 0.995), which was significantly less than that for gelatin (3700 Ω, R-square = 0.981). The fitted capacitance in CPE for PPY-CHI was 1.06 μF (R-square = 0.995), which was significantly larger than for gelatin (0.52 μF, R-square = 0.981). The corresponding permittivity (ε) of PPY-CHI was also significantly higher than for gelatin (2.70×10^{-5} F/m vs. 1.33×10^{-5} F/m), (Supplementary Figs. 1a–d). Therefore, the PPY-CHI interface was easier to polarize, allowing for more effective conduction of electrical signals generated by the heart tissue.

3.3. Conductive biomaterial facilitated scar electrical conduction, increased regional scar field potential, and reduced myocardial fibrotic tissue resistance

To evaluate the effect of PPY-CHI on cardiac scar/fibrotic tissue electrical activity and tissue resistance *in vivo*, a rat MI model was generated by coronary artery ligation, and PPY-CHI was injected into the resulting fibrotic scar in the left ventricular free wall 7 days later. Twelve weeks following implantation, PPY-CHI (black in color, Fig. 3a, lower panel) was observed in the fibrotic tissue. A 36-lead flexible MEA was used to evaluate regional electrical field potentials and detect electrical impulse propagation across the scar area during heart contraction, while rats were under general anesthesia (Fig. 3a). PPY-CHI-injected hearts had greater field potential amplitude in the scar region, compared with infarcted hearts injected with CHI alone (Fig. 3b and c). In the current study, we were unable to measure the electron activity. Instead, we used the electrical field potential amplitude to monitor the conductive current in the tissue. Our finding suggested that the electric field potential generated by PPY-CHI is enough to excite the surrounding myocardium. Representative MEA color map images of the infarcted myocardium from both CHI control and PPY-CHI groups illustrate the propagation of electrical current across the scar region (Fig. 3d and e). In CHI-injected hearts, the current failed (only propagated halfway) to enter the scar region (Fig. 3d), while in PPY-CHI-injected hearts, conductive propagation progressed through the scar region (Fig. 3e). The conduction velocity (CV) of the myocardial fibrotic tissue with PPY-CHI was faster than for CHI (Fig. 3f). To explore the mechanism of operation, tissue resistance in fibrotic scar areas was measured using a resistivity apparatus (Fig. 3g, insert). PPY-CHI-injected tissue resistivity was significantly lower than in saline- or CHI-injected tissue (Fig. 3g), which is in agreement with our *in vitro* study showing fibrotic matrix impedance reduction after the addition of conductive polymers into gelatin.

3.4. Injection of conductive biomaterial enhanced global scar tissue field potential amplitude and improved conduction velocity in vivo

Using an *in vivo* model, we further evaluated the conductive biomaterial ability to improve post-MI heart electrophysiological function. PPY-CHI, CHI, or saline was injected into the infarcted region 7

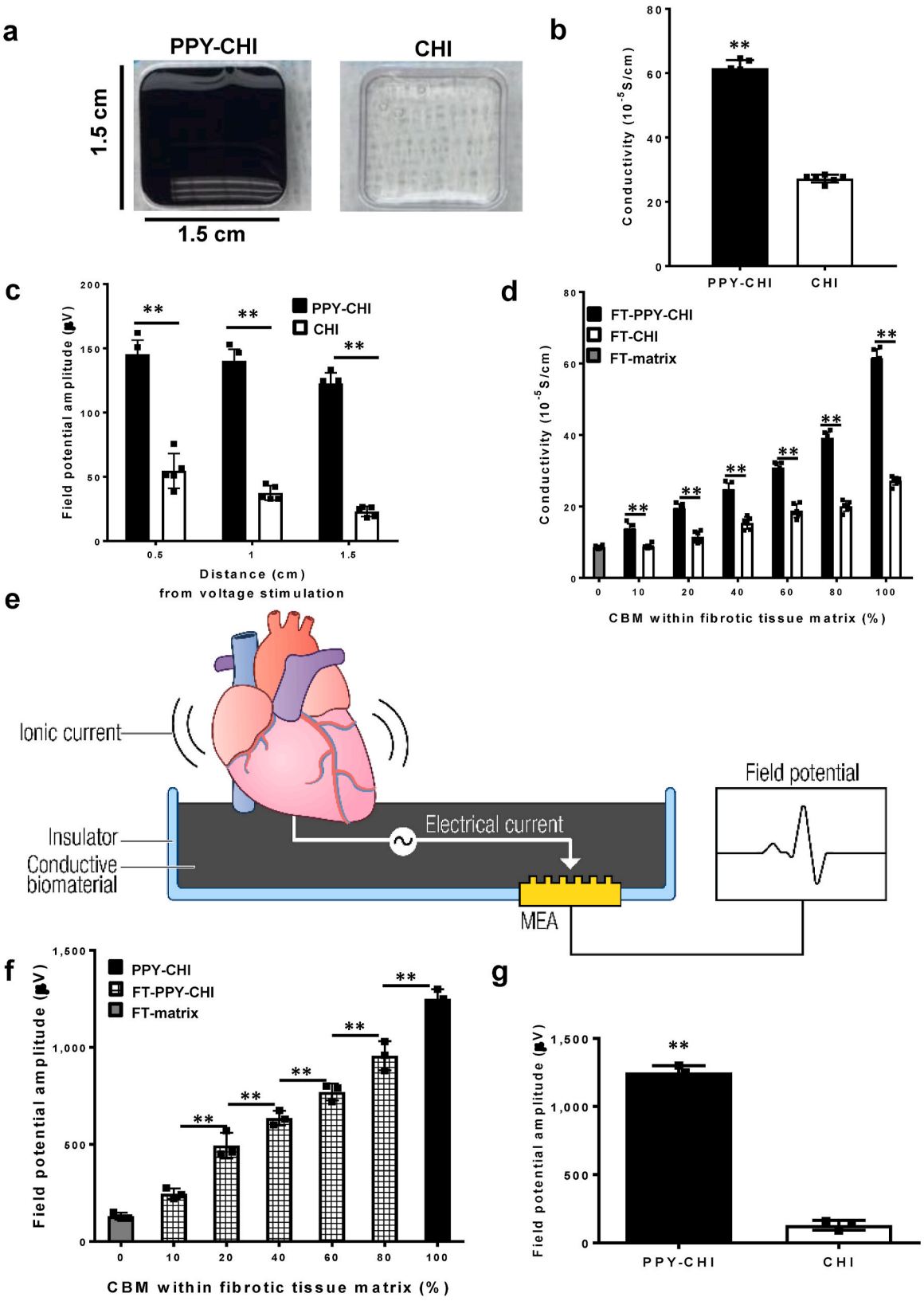

Fig. 1. Conductive biomaterial increased electrical conduction *in vitro* and *ex vivo*. **(a)** PPY-CHI and CHI hydrogel biomaterials. **(b)** Conductivity of biomaterials evaluated by the two-point probe method (n = 6/group). **(c)** Field potential amplitude was evaluated by the microelectrode array (MEA) method (n = 5/group). **(d)** Conductivity was measured by the two-point probe method in simulated fibrotic scar tissue (FT, 100% gelatin), with increasing proportions of conductive biomaterial (CBM) (n = 6/group). **(e)** A sealed system was created with a Langendorff-perfused beating heart on one side, and a MEA on the other side of the PPY-CHI cushion. **(f)** The field potential amplitude, detected by MEA, increased in a dose-dependent manner as the percentage of PPY-CHI within the matrix was increased (n = 3/group). **(g)** PPY-CHI had a 10-fold higher field potential amplitude compared to CHI. (n = 3/group) PPY = polypyrrole; CHI = chitosan.

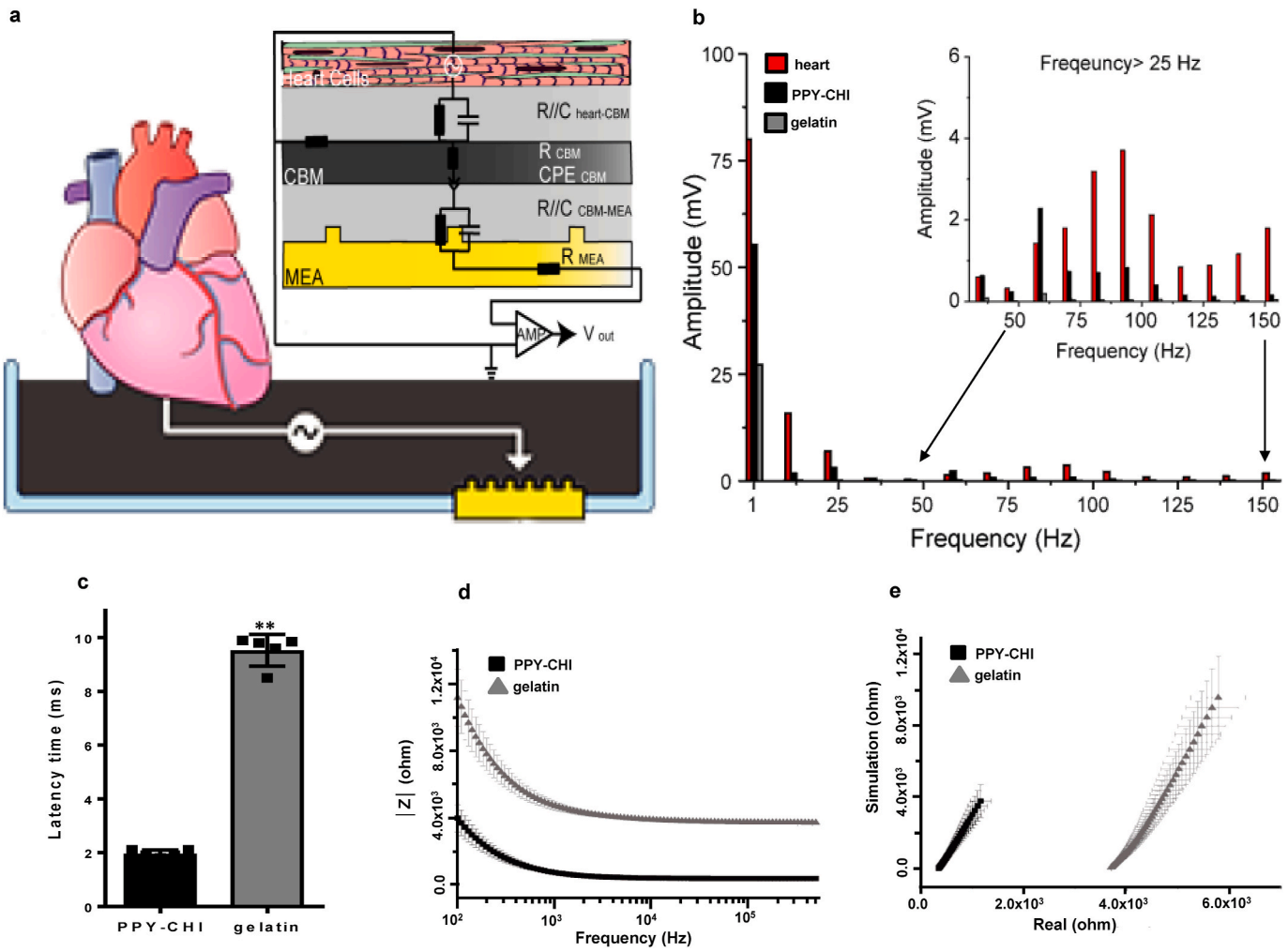

Fig. 2. Equivalent circuit model of biomaterials. (a) To quantify the difference in electrical parameters between conductive (PPY–CHI) and non-conductive (gelatin) biomaterials, an equivalent-circuit model of heart-material-microelectrode array (MEA) was established, and impedance measurements were taken. **(b)** Voltage decrease of an electrical current when passing through the equivalent circuit model for each biomaterial. The insert is a magnification of the amplitude from frequency 50–150 Hz. **(c)** Latency time of PPY-CHI and gelatin. **(d)** Bode plot, showing that the impedance of gelatin was higher than that of PPY-CHI in the whole frequency range. **(e)** Nyquist plot showing frequency responses, in the form of lines with different slopes, when PPY-CHI or gelatin is in the system (n = 5/group). PPY = polypyrrole; CHI = chitosan.

days after MI (Fig. 4a). PPY-CHI covered the whole scar area immediately after injection. Three-month post injection, PPY-CHI loci were still visible within the fibrotic tissue of the heart sections (Supplementary Figs. 2a–b). During the following 12 weeks, we assessed heart rate using echocardiogram (ECG), which was similar among the three groups before and after biomaterial injection (Fig. 4b). To evaluate the conductive properties of the post-treatment infarcted tissue, we employed 8-lead catheters to measure global cardiac surface field potential amplitude during cardiac contraction. Two leads were placed in normal myocardium, 2 leads in the border zone, and 2 leads in the fibrotic area (Fig. 4c and d). PPY-CHI-injected hearts had the highest scar field potential amplitude ratio (scar amplitude/remote amplitude), compared with saline- or CHI-injected infarcted hearts (Fig. 4e).

To directly assess electrical conduction velocity in the left ventricular free wall, we employed an optical mapping technique. Both healthy and infarcted hearts, which had been injected with saline, CHI, or PPY-CHI, were excised at 12 weeks post injection and perfused on a Langendorff perfusion system with a voltage-sensitive dye (di-4-ANEPPS). This was followed by a BDM (2, 3-butanedione monoxime) electromechanical uncoupler, in order to evaluate electrical impulse conduction velocity across both normal and infarct scar regions (Fig. 4f–i). Both saline and CHI-injected hearts had significantly decreased longitudinal conduction velocity, compared to normal hearts (Fig. 4j). However, the longitudinal conduction velocity of PPY-CHI-injected hearts was similar to healthy hearts, and was significantly greater than that of saline or CHI-injected hearts, indicating that the PPY-CHI injection improved post-injury cardiac electrical signal conduction (Fig. 4j).

3.5. *Conductive biomaterial shortened QRS/QT intervals and reduced ventricular arrhythmias*

To evaluate heart rhythm, 72 h of continuous recording was carried out under ambulatory telemetric ECG. At 12 weeks post treatment, infarcted animals showed frequent premature ventricular contractions (PVCs, Fig. 5a and b), though the PVC per hour frequency was lowest in the PPY-CHI group (Fig. 5b). To understand the mechanism, we analyzed the ECG data. ECGs (−1 week) obtained pre-MI showed normal baseline cardiac electrical activity. One week following MI (week 0), all rats exhibited a 50–80% prolongation of their QRS/QT intervals compared to pre-injury baseline values, indicating that MI disrupted normal electrical signal propagation (Fig. 5c–e). However, as early as 2 weeks after treatment, PPY-CHI-injected rats demonstrated significantly shorter QRS and QT intervals, compared to saline and CHI-injected animals. At 12 weeks, PPY-CHI-injected rats demonstrated 20–30%

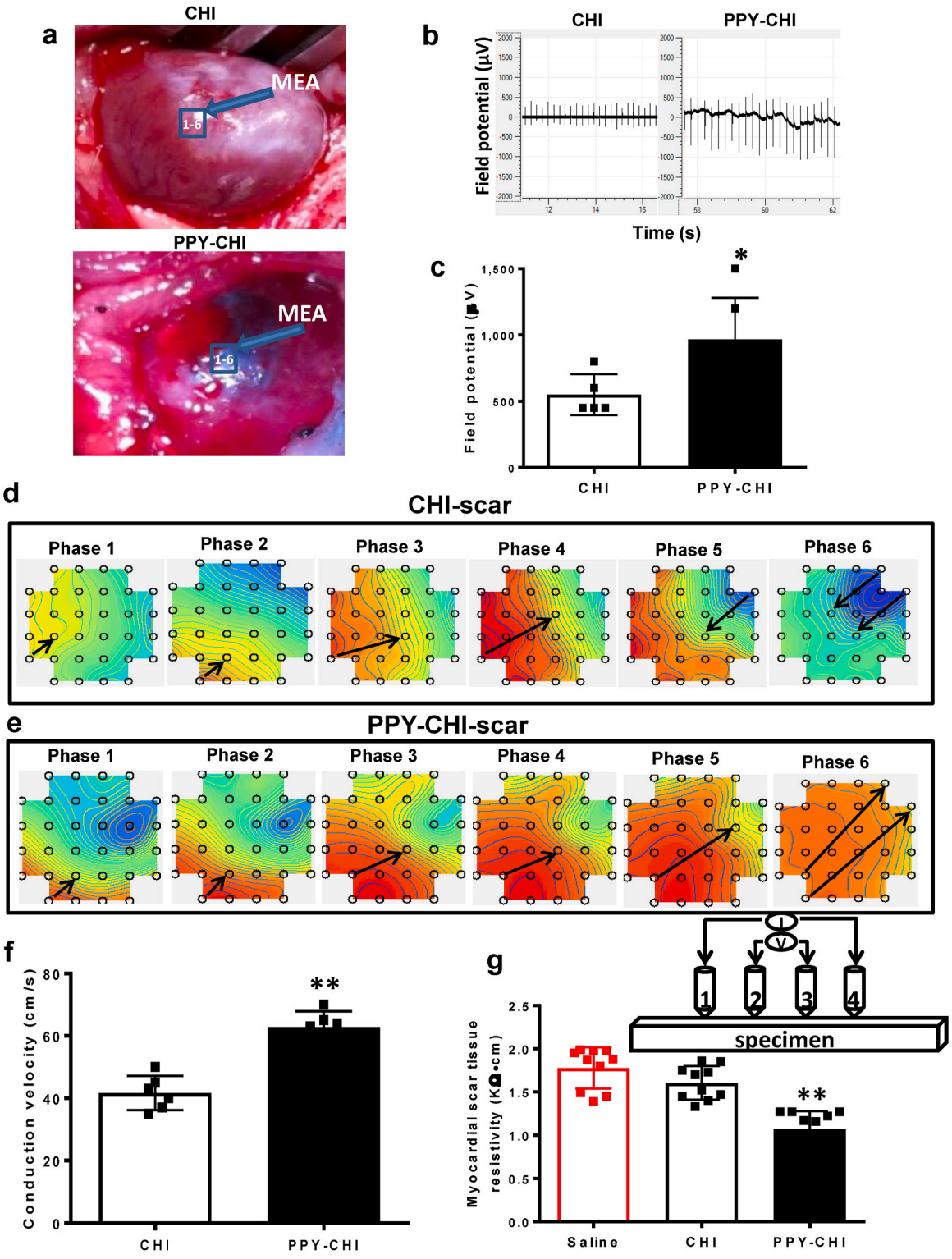

Fig. 3. Injection of PPY-CHI increased regional field potential amplitude and facilitated electrical current across scar. **(a)** Myocardial infarction was generated by coronary artery ligation, and either CHI or PPY-CHI was injected into the resulting fibrotic scar on the left ventricular free wall. PPY-CHI (black in color, lower panel) was observed in the fibrotic tissue. A microelectrode array (MEA) was used to evaluate regional electrical activity and conduction. **(b)** Representative scar field potential MEA images taken 12 weeks after biomaterial injection. **(c)** The field potential amplitude was significantly higher in PPY-CHI, compared with CHI-injected hearts (n = 5 for CHI and 6 for PPY-CHI). **(d–e)** Representative MEA images taken 12 weeks post-injection illustrate the propagation of electrical current across the scar region. **(f)** Conduction velocity evaluated by MEA was significantly higher in PPY-CHI, compared with CHI-injected hearts (n = 6/group). **(g)** Tissue resistivity was significantly lower in PPY-CHI, compared with saline- or CHI-injected hearts. Insert illustrates the four-probe method used to measure tissue resistivity (n = 10/group). *$P < 0.05$; **$P < 0.01$; PPY = polypyrrole; CHI = chitosan. . (For interpretation of the references to color in this figure legend, the reader is referred to the Web version of this article.)

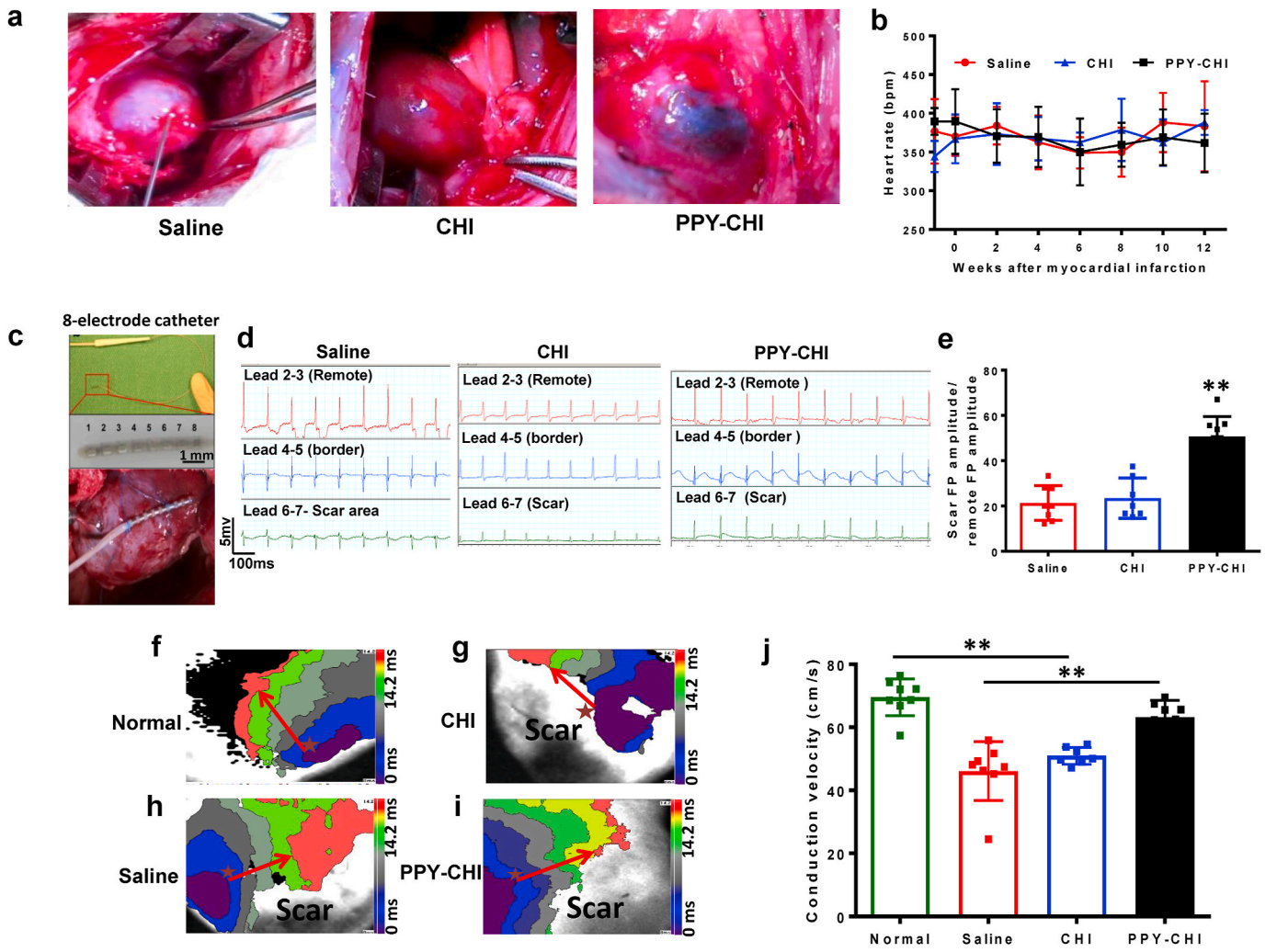

Fig. 4. Injection of PPY-CHI increased global field potential amplitude and improved conduction velocity. **(a)** Representative images taken after biomaterials or saline injection into the cardiac scar area. **(b)** Influence of biomaterials or saline injection on heart rate (n = 6/group). **(c)** Eight-lead catheters were used to measure global cardiac surface field potential amplitude. **(d)** Representative field potential images of remote, border and scar area, taken 12 weeks after biomaterials or saline injection. **(e)** The scar field potential amplitude ratio (scar amplitude/remote amplitude) was significantly higher in PPY-CHI, compared with saline- or CHI-injected hearts (n = 8 for saline, 7 for CHI and 9 for PPY-CHI). **(f–i)** Representative optical mapping images, taken 12 weeks post-injection. **(j)** Conduction velocity evaluated by optical mapping was significantly higher in PPY-CHI, compared with saline- or CHI-injected hearts, and was close to that of the normal heart (n = 8 for normal, saline and PPY-CHI, 6 for CHI). $^{**}P < 0.01$; PPY = polypyrrole; CHI = chitosan; FP = field potential.

shorter QRS and 50–60% shorter QT intervals, compared to saline and CHI-injected animals (Fig. 5d and e). The narrower QRS and QT intervals suggest a more efficient conduction in post-MI hearts treated with PPY-CHI than CHI or saline, which may have contributed to the decreased PVC number.

To investigate whether the conductive biomaterial reduced infarcted heart susceptibility to sustained ventricular arrhythmias, programmed electrical stimulation (PES), the standard clinical method for inducing arrhythmia, was used on post-MI rats 12 weeks following treatment (Fig. 5f). There, the post-PES arrhythmia susceptibility, as measured by the inducibility quotient, was significantly lower in PPY-CHI-injected rats compared to those injected with CHI or saline, which was suggestive of lesser arrhythmic susceptibility (Fig. 5g).

3.6. *Conductive biomaterial improved presumed synchronized contraction and preserved cardiac function following MI*

PPY-CHI, CHI, or saline-injected hearts were assessed using echocardiography at pre-injury (week −1), implantation (week 0) and up to 12 weeks post treatment (Fig. 6a). All groups showed reduced left ventricular fractional shortening (LVFS) and ejection fraction (LVEF), as well as increased LV internal systolic dimension (LVIDs) after treatment relative to pre-injury (Fig. 6b). However, CHI demonstrated a partial improvement, compared to saline, for these parameters at 12 weeks post-injection. Further improvement was found among PPY-CHI recipients, where significantly greater FS and EF, along with lower LVIDs, when compared to saline or CHI controls, was observed on week 12 post-treatment (Fig. 6b). Both CHI and PPY-CHI hearts may have benefited via them both having restricted dilatation; however, the lower LVIDs in the PPY-CHI group suggests that the improvement over the saline- or CHI- injected hearts may be more owed to reduction in cardiac dilatation, probably due to improved synchronized contraction.

Ventricular volumes and cardiac function were also evaluated by pressure-volume analysis. In agreement with the echocardiogram analysis, CHI rats showed improvements in cardiac function, including dP/dt Max and dP/dt Min, compared to saline controls 12 weeks after injection, while PPY-CHI-injected rats demonstrated even further improvement (Fig. 6c–f). Compared with saline, CHI rats resulted in lower end-systolic volume, which was further improved for PPY-CHI (Fig. 6g), indicating greater global contraction and improvement in systolic

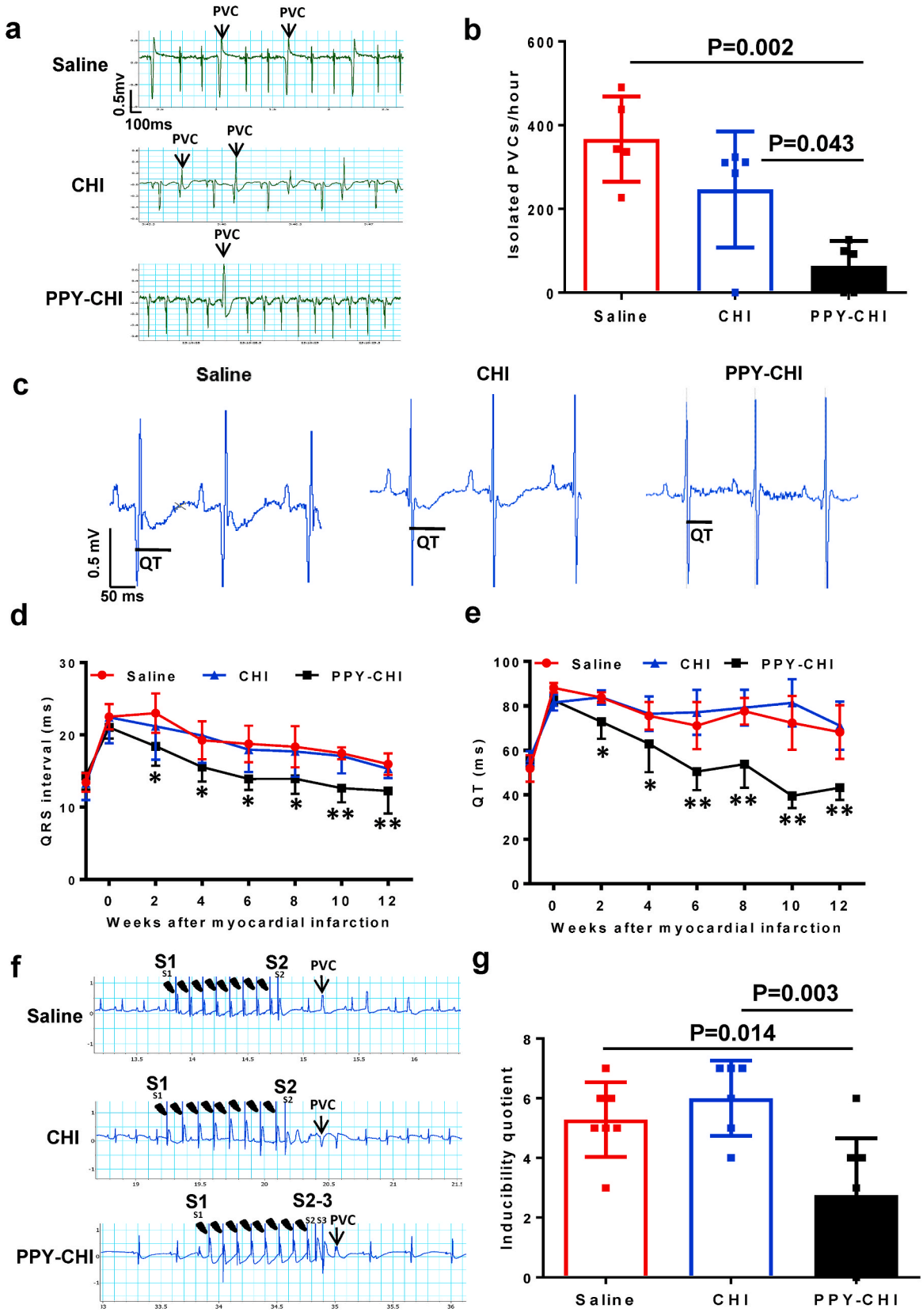

Fig. 5. Injection of PPY-CHI shortened QRS/QT intervals and reduced the rate of spontaneous and induced arrhythmias. **(a)** Representative telemetric ECGs showing premature ventricular contractions (PVCs). **(b)** Frequency of isolated PVCs, showing that PPY-CHI-injected hearts had the lowest hourly rate of PVCs (n = 5/group). **(c)** Representative surface echocardiograms (ECGs), taken 12 weeks post-injection. **(d–e)** Influence of biomaterial injection on QRS and QT complexes (n = 6/group). **(f)** Representative programmed electrical stimulation (PES)-induced ECGs showing arrhythmias. S1 = 8 burst stimulations; S2 = single extra-stimulus; S3 = double extra-stimuli **(g)** Arrhythmia susceptibility was determined by the inducibility quotient, and PPY-CHI-injected hearts had a significantly lower quotient (n = 7 for saline, 6 for CHI and 8 for PPY-CHI). *$P < 0.05$, **$P < 0.01$; PPY = polypyrrole; CHI = chitosan.

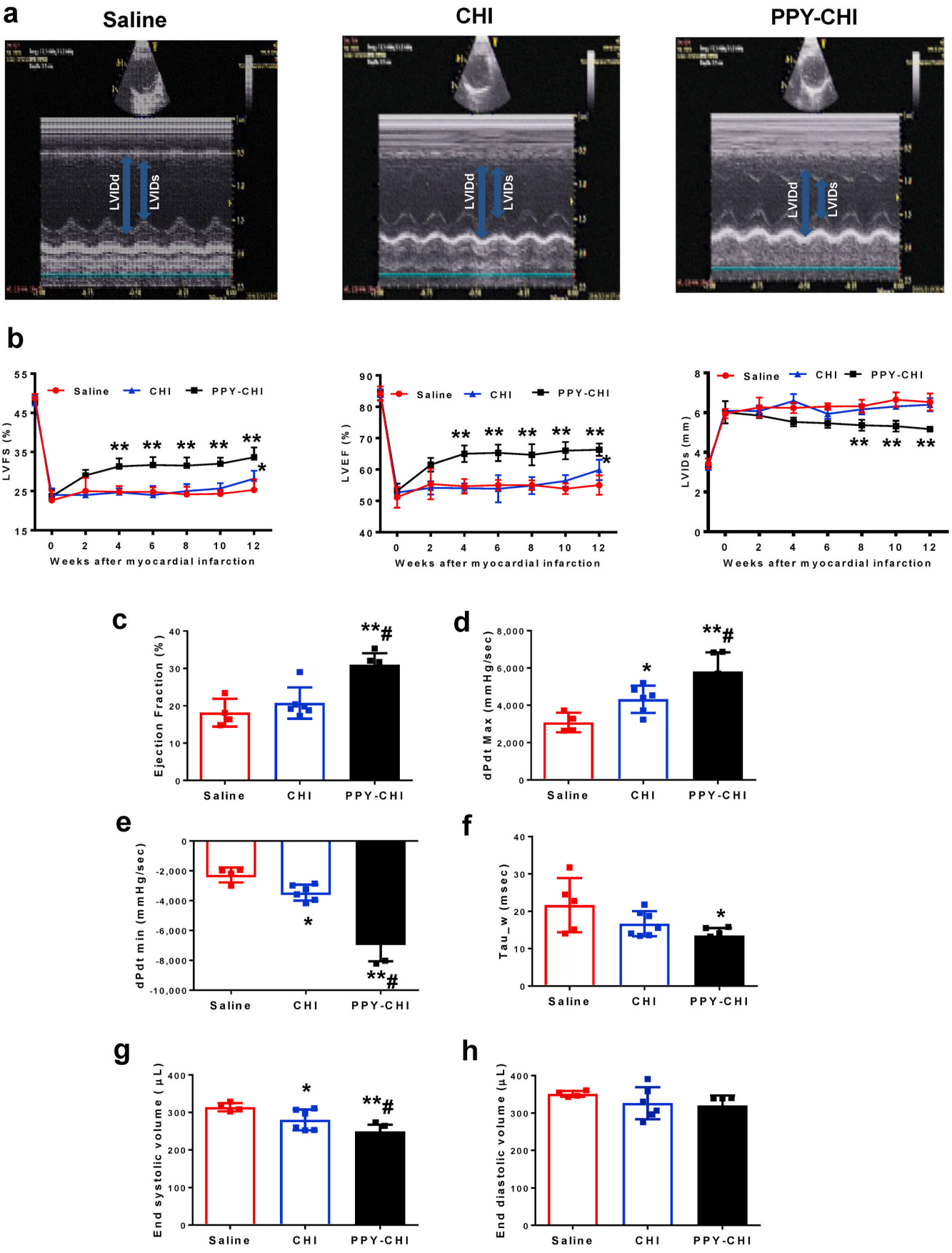

(caption on next page)

Fig. 6. Cardiac function was improved after PPY-CHI hydrogel injection into the scar zone. Saline, CHI or PPY-CHI was injected into the scar zone of rats 1 week post-MI. Echocardiography (echo) was performed at the time of MI (−1), the time of injection (0), and 2, 4, 6, 8, 10 and 12 weeks post-injection. **(a)** Representative 2D echo images 12 weeks after biomaterial injection, showing the left ventricular internal systolic (LVIDs) and left ventricular internal diastolic dimensions (LVIDd). (**b**) Comparison of mean fractional shortening and ejection fraction among experimental groups, which revealed significant improvements for CHI and PPY-CHI compared to saline alone at 12 weeks post-injection, with further improvement in function in PPY-CHI-injected animals ($^{*}P < 0.05$ and $^{**}P < 0.01$ vs saline respectively). PPY-CHI group also had the smallest LVIDs ($^{**}P < 0.01$) (n = 6/group). **(c–f)** Volumetric data taken using pressure–volume (P–V) analysis at 12 weeks post-injection showed that dPdt Max **(d)** and dPdt Min **(e)** improved significantly after injection with CHI compared to saline control, and these parameters along with % ejection fraction**(c)** and Tau **(f)** were further improved in animals injected with PPY-CHI (n = 4 for saline, 6 for CHI and 5 for PPY-CHI, $^{*}P < 0.05$ and $^{**}P < 0.01$ vs saline respectively, $\#P < 0.05$ vs CHI). Systolic volume was significantly lower in CHI compared with saline group, with further reduction in PPY-CHI injected animals (**g**, $^{*}P < 0.05$ and $^{**}P < 0.01$ vs saline respectively, $\#P < 0.05$ vs CHI). There were no significant changes in diastolic volume among the groups **(h)**. (n = 4 for saline, 6 for CHI and 5 for PPY-CHI) CHI = chitosan; PPY-CHI = polypyrrol-chitosan.

function. There were no differences in end-diastolic volume among the three groups (Fig. 6h).

Furthermore, we have previously published data showing that injection of chitosan into the damaged myocardium reduced scar size and increased scar thickness compared to saline control, leading to increased fibrotic tissue strength that may help to prevent fibrotic tissue thinning and expansion, allowing preservation of cardiac function [10].

Histological analysis identified the existence of PPY-CHI loci, showing them colored black within the fibrotic tissue of the heart sections at 3 months post conductive biomaterial injection (Supplementary Figs. 2a–b). Immunohistochemical staining was performed to evaluate angiogenesis in the three experimental groups. We found that the α-SMA positive area, an index for arteriogenesis, is significantly larger in the CHI and PPY-CHI than in saline-injected hearts (Supplementary Figs. 2c–d). Our data is in agreement with previously published data showing that PPY increased arteriole density, an indicator of angiogenesis, in an acute rat myocardial infarct model [16].

Taken together, these functional results suggest that injection of PPY-CHI post-MI was able to better maintain heart function and improve synchronized contraction, compared to non-conductive biomaterial injection.

4. Discussion

Cardiovascular diseases are the leading cause of death worldwide. As normal electrical conduction is essential for a well-functioning heart, innovative strategies have been investigated to improve heart conduction after an infarction or to promote myocardial repair, such as gene therapy, cell transplantation, or biomaterials as tools for cardiac tissue engineering [17–20]. Since the recent discovery of conductive polymers, the application of this material to reconnect myocardial conduction has received attention [10,11].

In the current study, we introduced a conductive material into non-conductive fibrotic matrix/tissue, where such functional polymers can reduce fibrotic tissue resistance (in an inverse correlation with conductivity) in a dose-dependent fashion. We demonstrated that the conduction of conductive biomaterial was faster, and energy output greater, via reduced resistivity in our equivalent circuit model compared to non-conductive biomaterial. In the beating heart, conductive material injected into fibrotic scar tissue improved the electrical conduction velocity of the fibrotic tissue, shortened depolarization-repolarization times, and prevented post-MI heart dysfunction.

Myocardial structural or composition alteration modifies cardiac electrical impulse propagation. Post-MI myocardial fibrosis separates functioning cardiomyocyte regions, thereby increasing the distance between contracting myocardial tissue. This results in a circuitous electrical propagation that delays depolarization, resulting in synchronous contraction loss. On an ECG, the QRS interval represents myocardial depolarization, while the QT interval represents ventricular electrical depolarization and repolarization. Widened QRS complexes and prolonged QT intervals are usually the result of intraventricular conduction defects. In our established animal model, we observed myocardial fibrosis and delayed electrical propagation, with post-MI yielding wider QRS and prolonged QT intervals. Introducing PPY-CHI into fibrotic tissue was able to reduce its impedance, and improved electrical conduction. MEA data demonstrated that myocardial electrical propagation can pass through the infarcted scar tissue after PPY-CHI addition, which was not possible in fibrotic tissue with CHI alone. PPY-CHI also improved the conductive velocity of the infarcted region in the left ventricular free wall, as our imaging studies have shown. This may be a possible mechanism for the shortened QRS/QT intervals observed after PPY-CHI treatment. These data demonstrate that the PPY-CHI hydrogel greatly reduced fibrotic scar tissue resistivity, compared with control materials.

Mechanistically, we investigated the latency time and energy decrease of an electrical current generated by cardiac tissue, passing through the conductive material in an equivalent circuit. The latency time was more than 5-fold shorter for PPY-CHI compared with non-conductive gelatin, indicating that the conduction velocity of an electrical current passing through PPY-CHI was significantly faster than that passing through the scar tissue-mimicking gelatin. Power spectrum analysis revealed that the energy that remained after passing through PPY-CHI at 1 Hz was >2 times greater than gelatin. This suggests that the biological current generated by the myocardium not only inducted electric current in the conductive material with less resistance at the interface, but also that PPY-CHI energy loss was significantly lower than that of gelatin.

One of the concerns with conductive biomaterial injection into an infarct scar is an increased susceptibility to ventricular arrhythmia, associated with alterations of ventricular depolarization patterns of the surrounding tissue. However, our *in vivo* telemetered ECG data demonstrated that PPY-CHI did not result in excessive ventricular arrhythmia during the 12-week experiment duration. This could be because the conductive velocity of the conductive biomaterial was slightly lower than that of the normal myocardium, though the difference was not statistically significant. Our programmed electrical stimulation results confirmed that substantially lower incidence of induced and spontaneous arrhythmias in conductive material-injected animals were present in PPY-CHI, compared to CHI or saline-injected controls. These data provide reassurance about the arrhythmogenic risk of cardiac repair with biomaterial injection, which is in agreement with prior studies showing that hydrogel injection into interstitial space does not impede electrical propagation [21]. Possible reasons for the reduced occurrence of arrhythmias could be the increased conduction velocity, or reduced tissue impedance in the scar tissue caused by the conductive polymers [22].

Cardiac resynchronization therapy (RT) has become the recommended treatment following an MI in patients with poor ventricular function and a prolonged QRS interval [23]. It has been shown to reduce heart failure mortality [4–6]. Biventricular pacing is now the recommended therapy for millions of survivors of extensive MI. Although the concept of electrical resynchronization is well established, limitations are present in the current methods. For example, cardiac RT has not been uniformly successful, even for patients with appropriate indicators. While cardiac RT is the established therapeutic option for advanced heart failure patients, a significant rate of non-responders has been repeatedly demonstrated [4,6,7]. Positioning the left ventricular lead near viable myocardium adjacent to the infarct is not possible in some

patients, due to variations in coronary venous anatomy [7]. Biomaterial injection has been demonstrated to preserve ventricular function post-MI [17–19,21]. Multiple mechanisms have been proposed for the beneficial effects of the injected biomaterial [17–19,21], and many enhancements have been proposed [17,19,20]. We proposed that the addition of a conductive polymer to the injectable biomaterial would provide substantial synergistic beneficial effects. We believe that the resulting enhancement of the impulse propagation across the fibrotic scar, leading to the shortening of the QRS interval, along with improving the synchronous contraction of the viable myocardium adjacent to the infarct scar, is a novel approach for improving recovery from a coronary occlusion.

In summary, we believe that several mechanisms are involved with respect to the contribution of PPY-CHI in restoring cardiac function, mainly through improving the conductive velocity of fibrotic tissue to enhance cardiac synchronized contraction, increasing scar thickness to prevent ventricular dilation, and inducing angiogenesis at the damaged tissue to reduce ischemic injury. Through MEA analysis, we proved that PPY-CHI-injected hearts had greater field potential amplitude and faster conduction velocity in the scar region. This was correlated with reduced fibrotic scar resistivity, compared with infarcted hearts injected with CHI alone. Using an 8-lead catheter for global filed potential measurement, we demonstrated that PPY-CHI-injected hearts had the highest scar field potential amplitude ratio (scar/remote amplitude), compared with saline- or CHI-injected infarcted hearts. Optical mapping with a voltage dye showed that the longitudinal conduction velocity of PPY-CHI-injected hearts was significantly greater than for saline or CHI-injected hearts, thereby serving as an indirect indicator of improved synchronized contraction in PPY-CHI injected hearts. ECG analysis showed that PPY-CHI shortened MI-induced prolonged QRS/QT intervals. Results obtained from ambulatory telemetric ECG and PES study showed that PPY-CHI could reduce hourly cardiac arrhythmia and post-PES arrhythmia susceptibility, as measured by the inducibility quotient, in PPY-CHI versus CHI or saline-injected hearts. All of these reductions were suggestive of lower arrhythmic susceptibility. Taken together, PPY-CHI hydrogel, with its superior conductive properties, reduced resistivity and enhanced electrical conduction across the fibrotic scar area, enhanced angiogenesis, was able to reduce the occurrence of cardiac arrhythmias, and synchronized cardiac contraction, ultimately leading to cardiac function improvement.

5. Conclusions

We dissected the mechanisms underlying the conductive biomaterial, PPY-CHI hydrogel, which has high *in vitro* conductivity and reduces tissue resistivity when injected into the fibrotic scar region of the infarcted heart. PPY-CHI improves conduction velocity and reduces arrhythmia susceptibility *in vivo*. We demonstrate that action potentials generated by beating Langendorff-perfused hearts can be converted to an electrical current in the conductive polymers. This biomaterial preserves cardiac function following MI and may offer a treatment for resynchronizing cardiac contraction in MI patients.

CRediT authorship contribution statement

Sheng He: Investigation, Writing - original draft, Formal analysis. **Jun Wu:** Methodology, Formal analysis. **Shu-Hong Li:** Methodology, Writing - review & editing. **Li Wang:** Investigation. **Yu Sun:** Investigation. **Jun Xie:** Conceptualization, Supervision. **Daniel Ramnath:** Methodology, Investigation. **Richard D. Weisel:** Conceptualization, Supervision. **Terrence M. Yau:** Conceptualization. **Hsing-Wen Sung:** Conceptualization. **Ren-Ke Li:** Conceptualization, Writing - review & editing, Funding acquisition.

Declaration of Competing Interest

The authors declare that they have no known competing financial interests or personal relationships that could have appeared to influence the work reported in this paper.

Acknowledgements

This work was supported by grants from the Collaborative Health Research Projects -Natural Sciences and Engineering Research Council of Canada and the Canadian Institutes of Health Research (523668 18 awarded to R. K. Li) and the Canadian Institutes of Health Research (332652 awarded to R. K. Li) and National Natural Science Foundation of China (81900274 awarded to Sheng He).

Appendix A. Supplementary data

Supplementary data to this article can be found online at https://doi.org/10.1016/j.biomaterials.2020.120285.

References

[1] K. Kikuchi, K.D. Poss, Cardiac regenerative capacity and mechanisms, Annu. Rev. Cell Dev. Biol. 28 (2012) 719–741.
[2] T.P. Nguyen, Z. Qu, J.N. Weiss, Cardiac fibrosis and arrhythmogenesis: the road to repair is paved with perils, J. Mol. Cell. Cardiol. 70 (2014) 83–91.
[3] D. Masarone, G. Limongelli, M. Rubino, F. Valente, R. Vastarella, E. Ammendola, R. Gravino, M. Verrengia, G. Salerno, G. Pacileo, Management of arrhythmias in heart failure, J Cardiovasc Dev Dis 4 (1) (2017).
[4] M.R. Bristow, L.A. Saxon, J. Boehmer, S. Krueger, D.A. Kass, T. De Marco, P. Carson, L. DiCarlo, D. DeMets, B.G. White, D.W. DeVries, A.M. Feldman, P. Comparison of Medical Therapy, I. Defibrillation, Heart Failure, Cardiac-resynchronization therapy with or without an implantable defibrillator in advanced chronic heart failure, N. Engl. J. Med. 350 (21) (2004) 2140–2150.
[5] W.T. Abraham, W.G. Fisher, A.L. Smith, D.B. Delurgio, A.R. Leon, E. Loh, D. Z. Kocovic, M. Packer, A.L. Clavell, D.L. Hayes, M. Ellestad, R.J. Trupp, J. Underwood, F. Pickering, C. Truex, P. McAtee, J. Messenger, Cardiac resynchronization in chronic heart failure, M.S.G.M.I.R.C. Evaluation, N. Engl. J. Med. 346 (24) (2002) 1845–1853.
[6] J.G. Cleland, J.C. Daubert, E. Erdmann, N. Freemantle, D. Gras, L. Kappenberger, L. Tavazzi, I. Cardiac Resynchronization-Heart Failure Study, the effect of cardiac resynchronization on morbidity and mortality in heart failure, N. Engl. J. Med. 352 (15) (2005) 1539–1549.
[7] J.M. Behar, T. Jackson, E. Hyde, S. Claridge, J. Gill, J. Bostock, M. Sohal, B. Porter, M. O'Neill, R. Razavi, S. Niederer, C.A. Rinaldi, Optimized left ventricular endocardial stimulation is superior to optimized epicardial stimulation in ischemic patients with poor response to cardiac resynchronization therapy: a combined magnetic resonance imaging, electroanatomic contact mapping, and hemodynamic study to target endocardial lead placement, JACC Clin Electrophysiol 2 (7) (2016) 799–809.
[8] R. Balint, N.J. Cassidy, S.H. Cartmell, Conductive polymers: towards a smart biomaterial for tissue engineering, Acta Biomater. 10 (6) (2014) 2341–2353.
[9] R.F. Service, Chemistry nobel: getting a charge out of plastics, Science 290 (5491) (2000) 425–427.
[10] A. Mihic, Z. Cui, J. Wu, G. Vlacic, Y. Miyagi, S.H. Li, S. Lu, H.W. Sung, R.D. Weisel, R.K. Li, A conductive polymer hydrogel supports cell electrical signaling and improves cardiac function after implantation into myocardial infarct, Circulation 132 (8) (2015) 772–784.
[11] Z. Cui, N.C. Ni, J. Wu, G.Q. Du, S. He, T.M. Yau, R.D. Weisel, H.W. Sung, R.K. Li, Polypyrrole-chitosan conductive biomaterial synchronizes cardiomyocyte contraction and improves myocardial electrical impulse propagation, Theranostics 8 (10) (2018) 2752–2764.
[12] M.J. Curtis, J.C. Hancox, A. Farkas, C.L. Wainwright, C.L. Stables, D.A. Saint, H. Clements-Jewery, P.D. Lambiase, G.E. Billman, M.J. Janse, M.K. Pugsley, G. A. Ng, D.M. Roden, A.J. Camm, M.J. Walker, The Lambeth Conventions (II): guidelines for the study of animal and human ventricular and supraventricular arrhythmias, Pharmacol. Ther. 139 (2) (2013) 213–248.
[13] T. Nguyen, E. El Salibi, J.L. Rouleau, Postinfarction survival and inducibility of ventricular arrhythmias in the spontaneously hypertensive rat : effects of ramipril and hydralazine, Circulation 98 (19) (1998) 2074–2080.
[14] J.G. Stinstra, B. Hopenfeld, R.S. Macleod, On the passive cardiac conductivity, Ann. Biomed. Eng. 33 (12) (2005) 1743–1751.
[15] A.A. Sagüés, S.C. Kranc, E.I. Moreno, Evaluation of electrochemical impedance with constant phase angle component from the galvanostatic step response of steel in concrete, Electrochim. Acta 41 (1996) 1239–1243.
[16] S.S. Mihardja, R.E. Sievers, R.J. Lee, The effect of polypyrrole on arteriogenesis in an acute rat infarct model, Biomaterials 29 (31) (2008) 4205–4210.
[17] J. Leor, S. Tuvia, V. Guetta, F. Manczur, D. Castel, U. Willenz, O. Petnehazy, N. Landa, M.S. Feinberg, E. Konen, O. Goitein, O. Tsur-Gang, M. Shaul, L. Klapper,

S. Cohen, Intracoronary injection of in situ forming alginate hydrogel reverses left ventricular remodeling after myocardial infarction in Swine, J. Am. Coll. Cardiol. 54 (11) (2009) 1014–1023.

[18] J. Leor, S. Aboulafia-Etzion, A. Dar, L. Shapiro, I.M. Barbash, A. Battler, Y. Granot, S. Cohen, Bioengineered cardiac grafts: a new approach to repair the infarcted myocardium? Circulation 102 (19 Suppl 3) (2000) III56–61.

[19] B. Deng, L. Shen, Y. Wu, Y. Shen, X. Ding, S. Lu, J. Jia, J. Qian, J. Ge, Delivery of alginate-chitosan hydrogel promotes endogenous repair and preserves cardiac function in rats with myocardial infarction, J. Biomed. Mater. Res. 103 (3) (2015) 907–918.

[20] K. Kang, L. Sun, Y. Xiao, S.H. Li, J. Wu, J. Guo, S.L. Jiang, L. Yang, T.M. Yau, R. D. Weisel, M. Radisic, R.K. Li, Aged human cells rejuvenated by cytokine enhancement of biomaterials for surgical ventricular restoration, J. Am. Coll. Cardiol. 60 (21) (2012) 2237–2249.

[21] N.J. Blackburn, T. Sofrenovic, D. Kuraitis, A. Ahmadi, B. McNeill, C. Deng, K. J. Rayner, Z. Zhong, M. Ruel, E.J. Suuronen, Timing underpins the benefits associated with injectable collagen biomaterial therapy for the treatment of myocardial infarction, Biomaterials 39 (2015) 182–192.

[22] H.G. Mond, J.R. Helland, K. Stokes, G.A. Bornzin, R. McVenes, The electrode-tissue interface: the revolutionary role of steroid-elution, Pacing Clin. Electrophysiol. 37 (9) (2014) 1232–1249.

[23] C. European Society of, A. European Heart Rhythm, M. Brignole, A. Auricchio, G. Baron-Esquivias, P. Bordachar, G. Boriani, O.A. Breithardt, J. Cleland, J. C. Deharo, V. Delgado, P.M. Elliott, B. Gorenek, C.W. Israel, C. Leclercq, C. Linde, L. Mont, L. Padeletti, R. Sutton, P.E. Vardas, ESC guidelines on cardiac pacing and cardiac resynchronization therapy: the task force on cardiac pacing and resynchronization therapy of the European Society of Cardiology (ESC). Developed in collaboration with the European Heart Rhythm Association (EHRA), Europace 15 (8) (2013) 1070–1118, 2013.